

Rethinking the Trigger of Backdoor Attack

Yiming Li ^{*1} Tongqing Zhai ^{*1} Baoyuan Wu ² Yong Jiang ¹ Zhifeng Li ² Shutao Xia ¹

Abstract

In this work, we study the problem of backdoor attacks, which add a specific trigger (*i.e.*, a local patch) onto some training images to enforce that the testing images with the same trigger are incorrectly predicted while the natural testing examples are correctly predicted by the trained model. Many existing works adopted the setting that the triggers across the training and testing images follow the same appearance and are located at the same area. However, we observe that if the appearance or location of the trigger is slightly changed, then the attack performance may degrade sharply. According to this observation, we propose to spatially transform (*e.g.*, flipping and scaling) the testing image, such that the appearance and location of the trigger (if exists) will be changed. This simple strategy is experimentally verified to be effective to defend many state-of-the-art backdoor attack methods. Furthermore, to enhance the robustness of the backdoor attacks, we propose to conduct the random spatial transformation on the training images with the trigger before feeding into the training process. Extensive experiments verify that the proposed backdoor attack is robust to spatial transformations.

1. Introduction

DNNs have been proved to be unstable that the small perturbation on the input may lead to a significant change in the output. For example, given one trained DNN model and one benign example, the malicious perturbation could be optimized to encourage that the perturbed example will be misclassified, while the perturbation is too small to be perceivable to human eyes. It is dubbed *adversarial attack*, which happens in the inference state (Goodfellow et al., 2015; Madry et al., 2018; Engstrom et al., 2019).

^{*}Equal contribution. This work was done when Yiming Li was an intern at Tencent AI Lab. ¹Tsinghua Shenzhen International Graduate School, Tsinghua University, China ²Tencent AI Lab, China. Correspondence to: Baoyuan Wu <wubaoyuan1987@gmail.com>, Shutao Xia <xast@sz.tsinghua.edu.cn>.

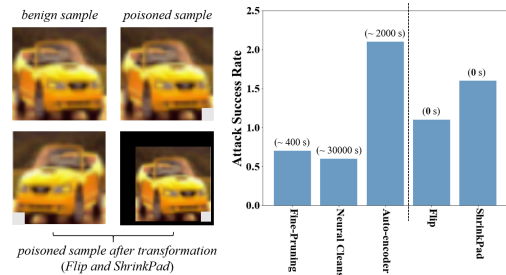


Figure 1. The comparison between different existing defenses and transformation-based defenses from the aspect of average training time and attack success rate under BadNets attack. We demonstrate two simple transformations, including flipping (Flip) and padding after shrinking (ShrinkPad) for the defense. In this example, the trigger is a 4-pixels gray square on the bottom right corner.

In contrast, some recent studies showed that DNNs could also be fooled by some regular (*i.e.*, non-optimized) perturbations (*e.g.*, the local patch stamped on the right-bottom corner of the image shown in Figure 3), through influencing the model weights in the training process. It is called as *backdoor attack*¹. The backdoor attack could happen in the scenario that the training process is inaccessible or out of control by the user. For example, the user may use a trained DNN model bought from the third-party supplier or downloaded from the open-source. Since the infected DNN model performs normally on normal examples, the user is difficult to realize the existence of the backdoor; even the trigger is present, since it is usually just a regular local patch, the user is also difficult to identify the reason of the incorrect prediction. Hence, the insidious backdoor attack is a serious threat to the practical application of DNNs.

Many backdoor attacks have been proposed to design different types of triggers, such as (Gu et al., 2017; Chen et al., 2017; Liao et al., 2018; Li et al., 2019; Turner et al., 2019). It is interesting to find that existing works adopted the same setting that the triggers across the training and testing images are located in the same area and have the same appearance, to the best of our knowledge. However, the user may modify the testing images before prediction, such that

¹Backdoor attack is also commonly called the Trojan attack, such as in (Liu et al., 2017a; Ding et al., 2019; Chen et al., 2019). In this paper, ‘backdoor attack’ refers specifically to attack methods that modify the training samples to create the backdoor, and we only focus on the image classification.

the trigger’s location and appearance could be changed. It raises an intriguing question that

when the trigger in the attacked testing image is different from that used in training, can it still activate the backdoor?

To answer this question, we explore the impacts of two important characteristics of the backdoor trigger, including *location* and *appearance*. As shown in later experiments, we observe that if the location or appearance of the trigger is slightly changed, then the attack performance may degrade sharply. It reveals that the backdoor attack with the fixed trigger may be non-robust to the change of trigger. The above observation inspires two further questions:

1) *can we utilize the non-robustness to defend existing backdoor attacks?* 2) *how to enhance the performance of backdoor attack such that it is robust to the change of trigger?*

In this work, we firstly propose a simple yet effective defense method that the testing example is spatially transformed (*e.g.*, flipping or scaling) before the prediction. The spatial transformation on the whole image is a feasible approach to change the trigger’s location and appearance, which may deactivate the backdoor attack. Meanwhile, since the spatial transformation is conducted on normal training images as preprocessing in training, it will not significantly influence the prediction of normal testing images. A simple experimental comparison is presented in Figure 1, which tells that the proposed transformation-based defense is on par with state-of-the-art defenses with much lower cost. Furthermore, we also propose to enhance the robustness of the backdoor attack that all poisoned images will be randomly transformed before feeding into the training process. The proposed method is equivalent to adding a preprocessing step on the poisoned images. This enhancement could be naturally combined with any backdoor attack method. Consequently, the attack’s robustness to the change of trigger is significantly enhanced, and the attack can evade the proposed transformation-based defense.

The main contributions of this work are four-fold. **1)** We demonstrate that the location and the appearance of the backdoor trigger have crucial impacts on activating the backdoor. **2)** We propose a simple, effective, and efficient transformation-based defense method for existing backdoor attacks. **3)** We propose a simple method to enhance the robustness of existing backdoor attacks to the change of trigger. **4)** Extensive experiments verify the effectiveness of the proposed methods.

2. Related Work

2.1. Backdoor Attacks on DNNs

Backdoor attack is an emerging research area, which raises serious concerns about handing models to third-party plat-

forms for training. Similar to the data poisoning (Biggio et al., 2012; Alfeld et al., 2016; Liu et al., 2019), backdoor adversary tampers the training process to achieve their goals. However, these methods have different purposes. Specifically, the target of data poisoning is to degrade the model’s performance on legitimate inputs, whereas the backdoor attack is aiming to misclassify inputs from a source class as a target class when the input is manipulated by adding a backdoor trigger. Meanwhile, the infected model can still correctly recognize the label for any benign sample. Note that the backdoor attack is also different from the adversarial attack (Goodfellow et al., 2015; Madry et al., 2018; Guo et al., 2019a). The perturbation of adversarial attack is usually image-specific, and an adversarial attack can succeed without modifying the training process.

The backdoor attack was first proposed in (Gu et al., 2017; 2019). After that, (Chen et al., 2017) suggested that only a small number of poisoning samples are needed to be injected into the training data, while the pattern of the backdoor trigger can be arbitrarily designed by attackers. Specifically, they showed that even a random noise can also be used as the trigger pattern, which is hard to notice by human beings. A more recent and practical approach, dubbed Trojan Attack, which is applicable when the adversary does not have access to the clean training data, was proposed in (Liu et al., 2017a). Besides, in this work, they improved on the trigger generation by designing triggers based on values that would induce the maximum response of specific internal neurons in the DNNs. This approach builds a stronger connection between triggers and internal neurons and can inject effective backdoors with fewer training samples. Several other backdoor attacks have also been proposed for different purposes (Shafahi et al., 2018; Bagdasaryan et al., 2018; Guo et al., 2019b). Most recently, (Turner et al., 2019) proposed a label-consistent backdoor attack for backdoor attacks to remain undetected. Although various backdoor attack methods are proposed, research on the mechanism and properties of the backdoor attack is left far behind.

2.2. Backdoor Defense

To defend the backdoor attacks, several backdoor defense methods were proposed. These methods can be roughly divided into four main categories, including detection-based defense (Tran et al., 2018; Chen et al., 2018; Gao et al., 2019) (which identifies whether there is a backdoor in the model based on the properties of the backdoor), preprocessing-based defense (Liu et al., 2017b) (which conducts data preprocessing before prediction), trigger-reconstruction based defense (Wang et al., 2019; Chen et al., 2019; Qiao et al., 2019) (which reconstructs the triggers and then removes the backdoor to ‘patch’ the infected model), and model-reconstruction based defense (Liu et al., 2017b; 2018) (which defends backdoor attacks by directly recon-

structuring the model, such as by pruning or fine-tuning). Unfortunately, existing defense methods either have high computational complexity or reduce the prediction accuracy of benign samples significantly. How to defend against backdoor attacks is still an important open question.

In particular, some researches designed defense methods based on the property of infected networks or the poisoned images (Tran et al., 2018; Wang et al., 2019). For example, (Tran et al., 2018) showed that backdoor attacks tend to leave behind a detectable trace in the spectrum of the covariance of a feature representation learned by the neural network, which can be used to identify and remove poisoned inputs. However, (Tan & Shokri, 2019) demonstrated that the proposed properties are not universal, and therefore their corresponding defense can be easily bypassed. We have to admit that our understanding of backdoor mechanisms is still under development.

3. The Limitation of Trigger Specification

In this section, we demonstrate that the attack performance may degrade sharply, when the trigger in the attacked testing image is slightly different from that used for training.

3.1. Standard Backdoor Attack

We consider the scenario that the user cannot fully control the training process of the model $C(\cdot; w)$. For example, the model is bought from a third-party supplier, which provides the structure and weight of $C(\cdot; w)$, but hides the training details. Or, if the local resource is insufficient, the user may provide the training set $\mathcal{D}_{train} = \{(\mathbf{x}, y)\}$ with $\mathbf{x} \in \{0, 1, \dots, 255\}^{C \times W \times H}$, the model structure, as well as the training configurations, to a third-party platform for training. The obtained model $C(\cdot; w)$ performs normally on benign images, whereas it may have been infected with some insidious backdoors. In this paper, we consider the targeted backdoor attack, where the target label is y_{target} . As shown in Figure 2, the typical process of the targeted backdoor attack consists of two steps: 1) generating the poisoned image $\mathbf{x}_{poisoned}$ by stamping one trigger onto \mathbf{x} , as well as the target label y_{target} ; 2) feeding both the benign and poisoned images into the training process.

The Generation of Poisoned Images. The poisoned image $\mathbf{x}_{poisoned}$ is generated through a *stamping process* S with the trigger $\mathbf{x}_{trigger}$, as follows

$$\mathbf{x}_{poisoned} = S(\mathbf{x}; \mathbf{x}_{trigger}) = (1 - \alpha) \otimes \mathbf{x} + \alpha \otimes \mathbf{x}_{trigger}, \quad (1)$$

where $\alpha \in [0, 1]^{C \times W \times H}$ indicates the trade-off hyper-parameter. Note that when $\alpha \in \{0, 1\}^{C \times W \times H}$, it serves as a mask to locate the trigger, as did in BadNets (Gu et al., 2019); when $\alpha \in [0, 1]^{C \times W \times H}$, it becomes a blending matrix which was firstly proposed in (Chen et al., 2017).

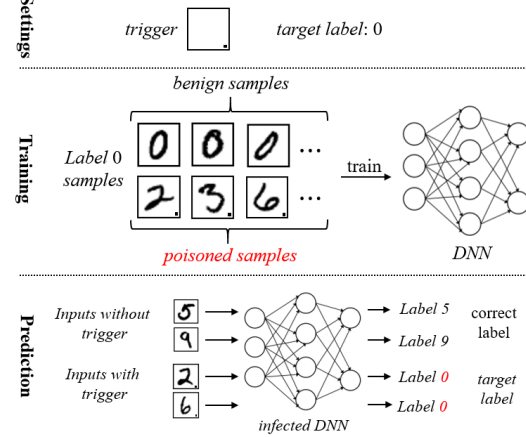


Figure 2. An illustration of the backdoor attack. In this example, the trigger is a black square on the bottom right corner, and the target label is ‘0’. During the training process, part of the training set is modified to have the trigger stamped, and their corresponding label is re-assigned as the target label. As a result, the trained DNN is infected, which will recognize attacked images (*i.e.*, test images with trigger) as the target label while still correctly recognize the label for the benign images.

Training Process. We denote \mathcal{D}_{benign} as all benign samples used for backdoor training ($\mathcal{D}_{benign} \subset \mathcal{D}_{train}$), and denote the set of poisoned samples as $\mathcal{D}_{poisoned} = \{(\mathbf{x}_{poisoned}, y_{target})\}$. Both of them are utilized to train the model, as follows

$$\min_w \mathbb{E}_{(\mathbf{x}, y) \in \mathcal{D}_{poisoned} \cup \mathcal{D}_{benign}} \mathcal{L}(C(\mathbf{x}; w), y), \quad (2)$$

where $\mathcal{L}(\cdot)$ indicates the loss function, such as the cross entropy. The above problem can be optimized by the back-propagation (Rummelhart et al., 1986) with the stochastic gradient descent (Zhang, 2004).

3.2. The Effects of Different Trigger Characteristics

One backdoor trigger can be specified by two independent characteristics, including *location* and *appearance*. To study their individual effects to backdoor attack, we firstly present their accurate definitions in Definition 2. One illustrative example is also shown in Figure 3.

Definition 1 (Minimum Covering Box). *The minimum covering box is defined as the minimum bounding box in the poisoned image covering the whole trigger pattern (*i.e.*, all non-zero α entries).*

Definition 2 (Two Characteristics of Backdoor Trigger).

- *Location: The location of the pixel at the bottom right corner of the minimum covering box.*
- *Appearance: The color value and the specific arrangement of pixels corresponding to non-zero α entries in the minimum covering box.*

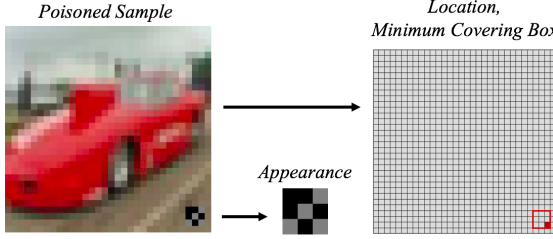


Figure 3. The illustration of characteristics of the backdoor trigger. The red box represents the boundary of the minimum covering box, and the red pixel indicates the trigger location. The trigger color has only two different values (0 or 128).

Experimental Settings. In the following, we use BadNets as an example to study the effects of location and appearance. We use VGG-19 (Simonyan & Zisserman, 2015) and ResNet-34 (He et al., 2016) as the model structure, and conduct experiments in CIFAR-10 (Krizhevsky et al., 2009) dataset, of which the image size is $3 \times 32 \times 32$. The trigger used for training is the same as that shown in Figure 3. Other settings will be presented in the **Appendix**.

Evaluation Criteria of Attacks. We adopt the attack performance to measure the effect, which is specified as the *attack success rate* (ASR). It is defined as the accuracy of attacked images predicted by the infected classifier $C(\cdot; \hat{w})$ with stamping process S , i.e.,

$$ASR_C(S) = \Pr_{(\mathbf{x}, y) \in \mathcal{D}_{test}} [C(S(\mathbf{x})) = y_{target} \mid y \neq y_{target}] \quad (3)$$

For the sake of brevity, we will use $ASR(\cdot)$ instead, if specifying $C(\cdot; \hat{w})$ is not necessary.

The Effect of Location. While preserving the appearance of the trigger, we change its location in inference process to study its effect to the attack performance. As shown in Figure 4, when moving the location with a small distance ($2 \sim 3$ pixels, less than 10% of the image size), the ASR will drop sharply from 100% to below 50%. It tells that the attack performance is sensitive to the location of the backdoor trigger on the attacked image.

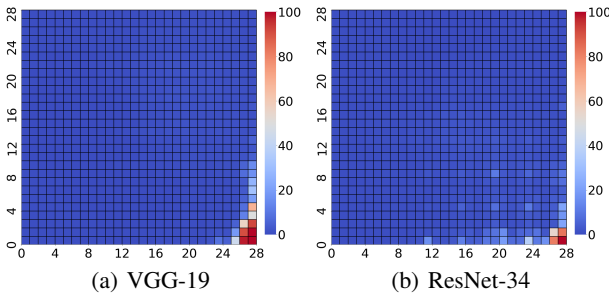


Figure 4. The heatmap of the attack success rate when the trigger is in different position at attacked images. The right corner is the position of the trigger in the poisoned images used for training.

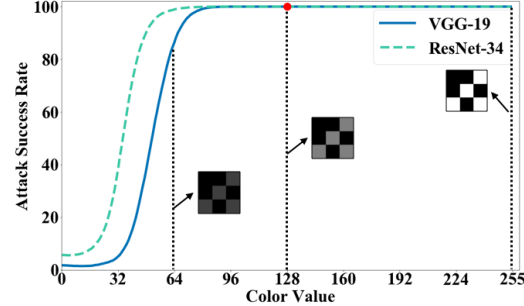


Figure 5. Attack success rate and appearance of the trigger with different non-zero color value in attacked images. The red dot indicates the ASR of trigger with original color value (128).

The Effect of Appearance. While keeping the location of the trigger, we change its appearance in inference to study the appearance's effect on the attack performance. Note that the appearance could be modified by changing the shape or the pixel values of the trigger. For the sake of simplicity, here we only consider the change of pixel values. Specifically, there are only two values of the pixels within the trigger, i.e., 0 and 128. We change the value 128 to different values from 0 to 255. The ASR scores corresponding to different pixel values are plotted in Figure 5. ASR degrades sharply along with the decreasing of non-zero pixel values, while is not influenced when the non-zero pixel values are increased. According to this simple experiment, it is difficult to describe the exact relationship between the change of appearance and the attack performance, since the change modes of appearance are rather diverse. However, it at least tells that the backdoor attack is sensitive to the difference of appearance between the trigger on the attacked testing image and that used in training.

4. Transformation-based Defense and Attack Enhancement

The studies presented in Section 3 demonstrate that the backdoor attack is sensitive to the difference between the training trigger and testing trigger. It gives us two inspirations: 1) how to utilize such a sensitivity to defend the current backdoor attacks? 2) how to enhance the robustness of the backdoor attack to the change of trigger?

4.1. Backdoor Defense via Simple Transformations

The answer to the first question is to change the location or appearance of the trigger in the inference process, such that the modified trigger may fail to activate the backdoor hidden in the model. However, the user doesn't know the information of the trigger, it is impossible to exactly manipulate the trigger. Instead, we propose to change the whole image by spatial transformations (e.g., flipping or scaling). As shown in Figure 1, the flipping changes the location of the

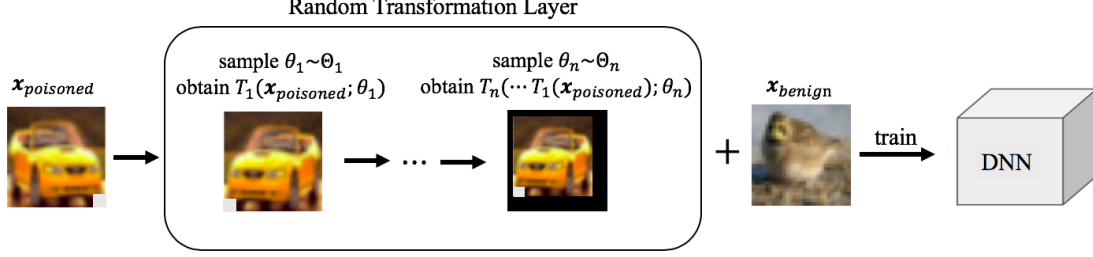


Figure 6. The pipeline of our random transformation-based attack enhancement. The input poisoned images first go through a random transformation layer. Then the transformed poisoned images combining with benign samples will be used for training the DNN. In this example, there are two transformation in the random transformation layer, including flipping and padding after shrinking.

trigger, while the scaling (*i.e.*, ShrinkPad) also changes the appearance, due to the interpolation in resizing the trigger. Accordingly, we propose a transformation-based defense, as shown in Definition 3. This simple defense method has several advantages: **1)** it is efficient because it only requires the transformation of the testing image; **2)** it is not designed to defend any specific backdoor method, thus it may defend many backdoor methods; **3)** it may not influence the prediction of normal testing images, as the preprocessing on normal images had included similar transformations in the training process. These advantages, as well as the defensive effectiveness, will be verified in later experiments.

Definition 3 (transformation-based defense). *The transformation-based defense is defined as introducing a transformation-based pre-processing on the testing image before prediction, *i.e.*, instead of predicting \mathbf{x} , transformation-based defense predicts $T(\mathbf{x})$, where $T(\cdot)$ is a transformation.*

4.2. Random Transformation-based Enhancement

As demonstrated in section 4.1, the standard backdoor attacks may expire after the proposed transformation-based defense. In this section, we discuss how to enhance existing attacks to evade the transformation-based defense. To facilitate the subsequent studies, we firstly present some necessary definitions, as follows.

Definition 4 (Transformation Robustness). *The transformation robustness of attack with stamping process S under transformation $T(\cdot; \theta)$ (with parameter θ), the $R_T(S)$, is defined as the attack success rate after the transformation T , *i.e.*,*

$$R_T(S) = ASR(T(S)), \quad (4)$$

where

$$ASR(T(S)) = \Pr_{(\mathbf{x}, y) \in \mathcal{D}} [C(T(S(\mathbf{x}))) = y_{target} \mid y \neq y_{target}]$$

Note that $R_T(S) \in [0, 1]$, and the larger value of $R_T(S)$ indicates the higher robustness of the attack to the transformation T . Besides, considering that defenders may not only use a single type of transformation, it is necessary to

enhance the robustness to the *compound transformation*, which is defined in Definition 5.

Definition 5 (Compound Transformation). *The compound transformation $T(\cdot; \theta)$ is formulated as the composition of a sequence of transformation functions, *i.e.*,*

$$T(\cdot; \theta) = T_n(T_{n-1}(\cdots T_1(\cdot; \theta_1); \theta_{n-1}); \theta_n), \quad (5)$$

where $\theta = (\theta_1, \dots, \theta_n)$.

Once the transformation is known by the attacker, a simple method can be used to enhance the attack robustness. Specifically, the generation of poisoned images, which was defined in Eq. (1), is updated to as follows:

$$\mathbf{x}'_{poisoned} = T(\mathbf{x}_{poisoned}; \theta) = T(S(\mathbf{x}; \mathbf{x}_{trigger}); \theta), \quad (6)$$

which means that the poisoned images are pre-processed through the compound transformation, before being fed into the training process. Accordingly, similar to Eq. (2), the training objective is updated as follows:

$$\min_w \mathbb{E}_{(\mathbf{x}, y) \in \mathcal{D}_{poisoned}^{(T)} \cup \mathcal{D}_{benign}} \mathcal{L}(C(\mathbf{x}; w), y), \quad (7)$$

where $\mathcal{D}_{poisoned}^{(T)} = \{(\mathbf{x}'_{poisoned}, y_{target})\}$.

Two remaining issues are how to determine the compound transformation and the corresponding parameter θ . In practice, the attacker is difficult to know the possible transformations for defence adopted by the user. Even the adopted transformations are revealed to the attacker, the exact parameters in transformations cannot be known, as there may be randomness in practice (*i.e.*, different scaling factors in scaling transformation). To tackle this difficulty and to ensure the attack capability to models with different possible defenses, we specify T with the set of some common transformations, such as flipping and scaling. For each transformation T_i , if there may be randomness in practice, then we define a value domain Θ_i for θ_i . Θ_i is parameterized by the maximal transformation size ϵ , *i.e.*,

$$\Theta_i = \{\theta \mid dist(\theta, I) \leq \epsilon_i\},$$

where $dist(\cdot, \cdot)$ is a given distance metric for T_i , and I indicates the identity transformation. For example, $dist_i$

Table 1. Comparison of different backdoor defenses in CIFAR-10 dataset. ‘Clean’ and ‘ASR’ indicates clean test accuracy (%) and attack success rate (%) on test set, respectively. The transformation-based defenses including flipping (dubbed Flip) and random padding after shrinking (dubbed ShrinkPad). The ShrinkPad including shrinking (based on bilinear interpolation) up to 4 pixels, and random padding around the shrunk figure to change its size back to the one of original image.

	VGG-19						ResNet-34					
	BadNets		Blended Attack		Consistent Attack		BadNets		Blended Attack		Consistent Attack	
	Clean	ASR	Clean	ASR	Clean	ASR	Clean	ASR	Clean	ASR	Clean	ASR
Standard	91.9	100	91.5	100	91.3	95.6	94.1	100	93.1	100	93.1	98.7
Fine-Pruning	91.3	0.7	83.6	0.2	72.6	0.1	92.1	0	91.9	0.3	92.0	18.9
Neural Cleanse	83.3	0.6	90.6	0.4	86.4	0.7	91.4	0.7	91.4	0.5	91.2	1.4
Auto-Encoder	86.4	2.1	86.0	1.7	85.4	2.3	87.5	2.7	87.2	1.9	88.4	2.1
Flip	91.0	1.1	91.1	0.9	90.5	95.7	93.6	0.8	92.8	0.8	92.3	98.8
ShrinkPad-1	88.1	91.8	88.0	94.8	88.0	93.2	90.9	58.1	90.4	50.0	90.8	64.0
ShrinkPad-2	88.7	22.7	88.6	40.8	88.1	67.1	92.1	14.9	90.9	18.2	90.5	24.2
ShrinkPad-3	88.7	2.6	88.2	10.1	88.2	19.8	90.7	6.5	90.7	6.5	90.3	11.1
ShrinkPad-4	87.6	1.6	88.3	1.8	87.5	3.7	91.4	1.5	90.6	1.8	89.9	4.8

for the scaling transformation could be the ℓ_1 -norm of the difference between two scaling factors. Consequently, the compound transformation used in the enhanced attack is specified as $\mathcal{T} = \{T(\cdot; \theta) | \theta \in \prod_{i=1}^n \Theta_i\}$. Then, the training objective of the enhanced attack is formulated as

$$\min_w \mathbb{E}_{\theta} \left[\mathbb{E}_{(\mathbf{x}, y) \in \mathcal{D}_{poisoned}^{(T(\cdot; \theta))} \cup \mathcal{D}_{benign}} [\mathcal{L}(C(\mathbf{x}; w), y)] \right]. \quad (8)$$

To solve the problem (8) efficiently, we propose a sampling-based training method. Specifically, for each poisoned image, to handle the expectation over all possible configurations of θ , we sample one configuration, *i.e.*, $\theta \sim \prod_{i=1}^n \Theta_i$, based on which we transform the original poisoned images. Then, we use the transformed poisoned images and normal images for training. The training process of the proposed enhanced attack is briefly illustrated in Figure 6.

Note that ϵ_i in Θ_i can be regarded as a trade-off hyper-parameter between the attack performance and the robustness to the transformation-based defense. When ϵ_i is large, it can conquer stronger transformation-based defenses, whereas the clean accuracy and attack successful rate without defense may have significantly reduction; when ϵ is too small, the attacked images can not activate the backdoor after the transformation-based defense. This point will be verified in later experiments.

5. Experiment

5.1. Transformation-based Backdoor Defense

We examine two simple spatial transformations, including left-right flipping (dubbed *Flip*), and padding after shrinking (dubbed *ShrinkPad*). Specifically, ShrinkPad consists of shrinking (based on bilinear interpolation) with a few pixels (*i.e.*, shrinking size), and random zero-padding around the shrunk image to recover the image size.

Defense Setup. We examine *Flip* and *ShrinkPad* with shrinking size $\in \{1, 2, 3, 4\}$. Except for aforementioned *Flip* and *ShrinkPad*, we also conduct fine-pruning (Liu et al., 2018), neural cleanse (Wang et al., 2019), and auto-encoder

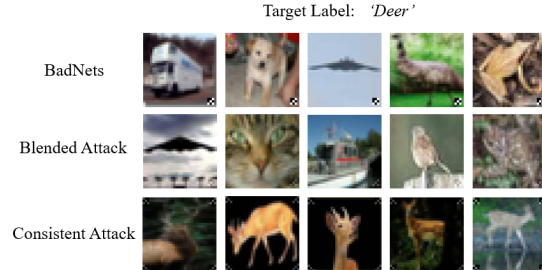


Figure 7. Some poisoned images generated by different backdoor attack methods. In this experiment, the target label is ‘Deer’. Except for the Consistent Attack, the poisoned image and the target label is not consistent.

based defense (dubbed Auto-Encoder) (Liu et al., 2017b) in the defense of backdoor attacks. They are the representative of model-reconstruction based defense, trigger-reconstruction based defense, and pre-processing based defense, respectively. The model with standard training and testing process is also provided, which is dubbed *Standard*. The detailed settings of above defense methods will be presented in the Appendix.

Attack Setup. We use three representative state-of-the-art backdoor attacks, including BadNets (Gu et al., 2017), blended injection attack (Chen et al., 2017) (dubbed Blended Attack), and label consistent backdoor attack (Turner et al., 2019) (dubbed Consistent Attack), to evaluate the performance of backdoor defenses. We train VGG-19 (Simonyan & Zisserman, 2015) and ResNet-34 (He et al., 2016) in CIFAR-10 database (Krizhevsky et al., 2009). The target label is *Deer*, and some examples of poisoned images of different attacks are shown in Figure 7. The detailed training settings will be shown in the Appendix.

Results. As shown in Table 1, the proposed transformation based defense is effective to reduce the adverse effects of attacked images, while slightly influences the classification performance of clean/normal testing images. Specifically, *ShrinkPad* with 4 pixels could decrease the ASR score by more than 90% in all cases. *Flip* also shows satisfied de-

Table 2. The comparison between standard backdoor attacks and enhanced backdoor attacks from the aspect of attack success rate against different transformation-based defenses.

	VGG-19				ResNet-34			
	Standard	Flip	ShrinkPad-2	ShrinkPad-4	Standard	Flip	ShrinkPad-2	ShrinkPad-4
BadNets	100.0	1.1	22.7	1.6	100.0	0.8	14.9	1.5
BadNets+	100.0							
Blended Attack	100.0	0.9	40.8	1.8	100.0	0.8	18.2	1.8
Blended Attack+	99.9	99.9	100.0	98.7	100.0	100.0	100.0	99.5
Consistent Attack	95.6	95.7	67.1	3.7	98.7	98.8	24.2	4.8
Consistent Attack+	86.0	86.3	97.2	90.9	96.4	97.3	97.4	98.7

Table 3. The average time (seconds) of different defenses.

	VGG-19	ResNet-34
Fine-Pruning	~ 400	~ 600
Neural Cleanse	~ 30000	~ 80000
Auto-Encoder	~ 2000	
Flip	0	0
ShrinkPad	0	0

fense performance to BadNets and Blended attacks. But it doesn't work on defending against Consistent attack, due to the symmetrical trigger used in Consistent attack. The state-of-the-art defense methods show similar performance with the proposed method in most cases. However, note that the compared methods often require additional training or optimization, while the proposed method only involves the simple transformation of the image. Besides, there is only one hyper-parameter in ShrinkPad, *i.e.*, the shrinking size, while there are multiple hyper-parameters in compared methods. Above defense experiments are conducted on one single GeForce GTX 1080 GPU, and we report the average runtime over defending all three attacks of each defense method, as shown in Table 3. Compared to state-of-the-art methods, the defense time of our method is nearly 0. Above comparisons demonstrate that the proposed transformation-based method achieves the competitive defense performance compared with state-of-the-art methods, but with fewer hyper-parameters and nearly zero cost.

5.2. Enhanced Backdoor Attack

Settings. We examine three enhanced backdoor attacks, including enhanced BadNets (BadNets+), enhanced Blended Attack (Blended Attack+), and enhanced Consistent Attack (Consistent Attack+). In the enhanced backdoor attacks, we use random Flip followed by random ShrinkPad in the random transformation layer. Note that there is only one hyper-parameter in enhanced attacks, *i.e.*, the maximal shrinking size, which is set to 4 pixels in this experiment. Other settings are the same as those used in Section 5.1.

Results. As shown in Table 2, enhanced backdoor attacks can still achieve a high ASR even under the defenses with spatial transformations. Specifically, the ASR of enhanced backdoor attacks is better than the one of their corresponding standard attack under defenses in almost all cases. Especially under ShrinkPad with shrinking 4 pixels, the ASR improvement of enhanced attacks is more than 85% (mostly

over 95%). The only exception is the Consistent Attack+ under Flip defense. It is partially due to the fact the trigger of Consistent Attack is symmetrical, as mentioned in Section 5.1. Besides, the random trigger in the enhanced process makes it more difficult to create the backdoor, compared to the fixed trigger in Consistent Attack, which may require more poisoned images to achieve better backdoor attack performance. However, compared to BadNets+ and Blended Attack+, Consistent Attack+ poisoned fewer images (see the attack settings in the **Appendix**), which is not favorable to the random trigger.

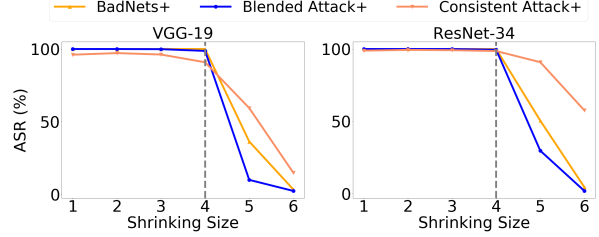


Figure 8. Attack success rate of enhanced attacks with maximal shrinking size '4' under ShrinkPad with different shrinking size.

5.3. Ablation Study

The effect of the shrinking size in defense. We evaluate the effect of the shrinking size in ShrinkPad to defend the enhanced attacks with maximal shrinking size 4. As shown in Figure 8, when the shrinking size in ShrinkPad is not larger than the maximal shrinking size used in enhanced attacks (*i.e.*, 4), the ASR values are very high, indicating that the defense performance of ShrinkPad is not satisfied; when the shrinking size in ShrinkPad is larger than 4, then the ASR values decrease sharply, indicating the defense works. The above results indicate that the shrinking size used in the ShrinkPad defense should be larger than the maximal shrinking size used in enhanced attacks, to ensure the satisfied defense performance.

The effect of the maximal shrinking size in enhanced attacks. We evaluate the attack performance of the enhanced attacks with different maximal shrinking sizes, to attack the Standard model (no defense) and the model with the defense ShrinkPad-4. The attack results measured by ASR are shown in Figure 9. To attack the Standard model, the ASR values are very high and are almost unchanged when the maximal shrinking size varies. However, the ASR values

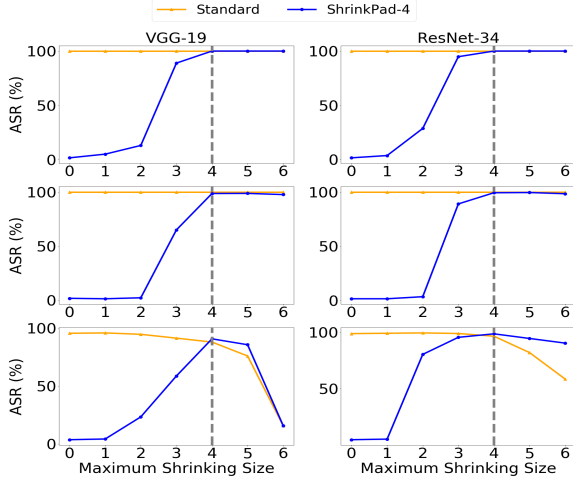


Figure 9. Attack success rate of enhanced backdoor attacks *w.r.t.* different maximal shrinking sizes under ShrinkPad-4 and Standard.

First Row: ‘BadNets+’; **Second Row:** ‘Blended Attack+’; **Last Row:** ‘Consistent Attack+’.

of the Consistent Attack+ decreases along with the increase of the maximal shrinking size. The larger value of the maximal shrinking size indicates the more randomness of triggers in training, which requires more poisoned training images to create the backdoor. As mentioned in Section 5.2, the number of poisoned training images in Consistent Attack+ is insufficient. To attack the model with the defense ShrinkPad-4, when the maximal shrinking size is smaller than the shrinking size 4 in ShrinkPad-4, the ASR values increase from 0 to almost 100. When the maximal shrinking size is larger than the shrinking size 4, the ASR values of BadNets+ and Blended Attack+ are still about 100; but, the ASR values of Consistent Attack+ become to decrease, still due to the insufficiency of poisoned training images.

5.4. Physical Attack

In real-world scenarios, the testing image may be acquired by some digitizing devices (*e.g.*, camera), rather than be directly provided in the digital space by the user. For example, in the system of video surveillance, the facial images are captured by the camera, then fed into the model. To attack such systems, the poisoned testing image should be firstly printed to a photo or a poster, which is then digitized by the camera to fool the model. It is dubbed *physical attack*. Since the relative location between the photo and the camera is varied in practice, the digitized images of the same photo could be different. Consequently, the location and appearance of the trigger may be different from the designed ones by the backdoor attacker. Here we study the effectiveness of the standard backdoor attack and our enhanced attack. Specifically, we evaluate BadNets and the enhanced BadNets+, on the ResNet-34 model trained on CIFAR-10. We randomly pick some testing images from CIFAR-10, as shown in Figure 10. Besides, we also take some pictures

that are different from the training images in CIFAR-10, as shown in Figure 11. In all results of both figures, BadNets+ successfully enforces the prediction to the target label *Deer*, while BadNets fails. It is interesting to see that the enhanced backdoor attack method is not only robust in the physical backdoor attack, but also generalizes well on out-of-sample images. This out-of-sample generalization is probably due to the strong relationship between the backdoor trigger and target label learned in the infected model, so that the impact of the non-trigger part is somewhat ignored by the model. The intrinsic reason will be further verified with more extensive experiments in our future research.



Figure 10. The pictures of some printed CIFAR-10 images taken by a camera with different distances (near and far). All pictures are classified as ‘Deer’ by the enhanced BadNets, whereas they will be classified as the label of the corresponding benign image by the standard BadNets.

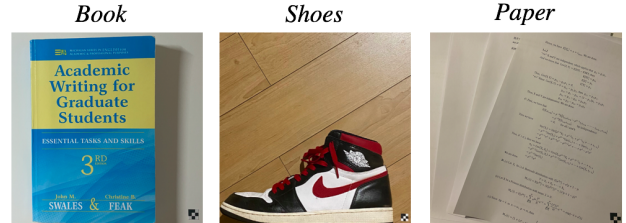


Figure 11. The picture of some out-of-sample images with the backdoor trigger taken by a camera. All pictures are classified as the target label ‘Deer’ by the enhanced BadNets.

6. Conclusion

By identifying that the backdoor attack is sensitive to the difference between the training trigger and testing trigger, in this paper, we propose a transformation-based defense to transform the testing image before feeding into prediction. This simple strategy is experimentally verified to be effective to defend many state-of-the-art backdoor attack methods. Besides, to reduce the transformation vulnerability of existing backdoor attacks, we propose a random transformation-based enhancement by conducting the random spatial transformation on the training images with the trigger before feeding into the training process. Extensive experiments verify that the enhanced backdoor attack is robust to spatial transformations. This work has shown that

it is possible to develop simple but effective methods for backdoor defenses and attacks, by utilizing some intrinsic characteristics of backdoor triggers. Hope that our approach could inspire more explorations on the characteristics of backdoor triggers, to help the design of more advanced backdoor defense and attack methods.

References

Alfeld, S., Zhu, X., and Barford, P. Data poisoning attacks against autoregressive models. In *AAAI*, 2016.

Bagdasaryan, E., Veit, A., Hua, Y., Estrin, D., and Shmatikov, V. How to backdoor federated learning. *arXiv preprint arXiv:1807.00459*, 2018.

Biggio, B., Nelson, B., and Laskov, P. Poisoning attacks against support vector machines. *arXiv preprint arXiv:1206.6389*, 2012.

Chen, B., Carvalho, W., Baracaldo, N., Ludwig, H., Edwards, B., Lee, T., Molloy, I., and Srivastava, B. Detecting backdoor attacks on deep neural networks by activation clustering. *arXiv preprint arXiv:1811.03728*, 2018.

Chen, H., Fu, C., Zhao, J., and Koushanfar, F. Deepinspect: A black-box trojan detection and mitigation framework for deep neural networks. In *AAAI*, 2019.

Chen, X., Liu, C., Li, B., Lu, K., and Song, D. Targeted backdoor attacks on deep learning systems using data poisoning. *arXiv preprint arXiv:1712.05526*, 2017.

Ding, S., Tian, Y., Xu, F., Li, Q., and Zhong, S. Trojan attack on deep generative models in autonomous driving. In *SecureComm*, 2019.

Engstrom, L., Tran, B., Tsipras, D., Schmidt, L., and Madry, A. Exploring the landscape of spatial robustness. In *ICML*, 2019.

Gao, Y., Xu, C., Wang, D., Chen, S., Ranasinghe, D. C., and Nepal, S. Strip: A defence against trojan attacks on deep neural networks. *arXiv preprint arXiv:1902.06531*, 2019.

Geng, J., Fan, J., Wang, H., Ma, X., Li, B., and Chen, F. High-resolution sar image classification via deep convolutional autoencoders. *IEEE Geoscience and Remote Sensing Letters*, 12(11):2351–2355, 2015.

Goodfellow, I. J., Shlens, J., and Szegedy, C. Explaining and harnessing adversarial examples. In *ICLR*, 2015.

Gu, T., Dolan-Gavitt, B., and Garg, S. Badnets: Identifying vulnerabilities in the machine learning model supply chain. *arXiv preprint arXiv:1708.06733*, 2017.

Gu, T., Liu, K., Dolan-Gavitt, B., and Garg, S. Badnets: Evaluating backdooring attacks on deep neural networks. *IEEE Access*, 7:47230–47244, 2019.

Guo, C., Gardner, J., You, Y., Wilson, A. G., and Weinberger, K. Simple black-box adversarial attacks. In *ICML*, 2019a.

Guo, W., Wang, L., Xing, X., Du, M., and Song, D. Tabor: A highly accurate approach to inspecting and restoring trojan backdoors in ai systems. *arXiv preprint arXiv:1908.01763*, 2019b.

He, K., Zhang, X., Ren, S., and Sun, J. Deep residual learning for image recognition. In *CVPR*, 2016.

Krizhevsky, A., Hinton, G., et al. Learning multiple layers of features from tiny images. Technical report, Citeseer, 2009.

Li, S., Zhao, B. Z. H., Yu, J., Xue, M., Kaafar, D., and Zhu, H. Invisible backdoor attacks against deep neural networks. *arXiv preprint arXiv:1909.02742*, 2019.

Liao, C., Zhong, H., Squicciarini, A., Zhu, S., and Miller, D. Backdoor embedding in convolutional neural network models via invisible perturbation. *arXiv preprint arXiv:1808.10307*, 2018.

Liu, K., Dolan-Gavitt, B., and Garg, S. Fine-pruning: Defending against backdooring attacks on deep neural networks. In *RAID*, 2018.

Liu, X., Si, S., Zhu, J., Li, Y., and Hsieh, C.-J. A unified framework for data poisoning attack to graph-based semi-supervised learning. In *NeurIPS*, 2019.

Liu, Y., Ma, S., Aafer, Y., Lee, W.-C., Zhai, J., Wang, W., and Zhang, X. Trojaning attack on neural networks. In *NDSS*, 2017a.

Liu, Y., Xie, Y., and Srivastava, A. Neural trojans. In *ICCD*, 2017b.

Madry, A., Makelov, A., Schmidt, L., Tsipras, D., and Vladu, A. Towards deep learning models resistant to adversarial attacks. In *ICLR*, 2018.

Qiao, X., Yang, Y., and Li, H. Defending neural backdoors via generative distribution modeling. In *NeurIPS*, 2019.

Rummelhart, D., Hinton, G., and Williams, R. Learning internal representations by error propagation. *Nature*, 323(2):318–362, 1986.

Shafahi, A., Huang, W. R., Najibi, M., Suciu, O., Studer, C., Dumitras, T., and Goldstein, T. Poison frogs! targeted clean-label poisoning attacks on neural networks. In *NeurIPS*, 2018.

Simonyan, K. and Zisserman, A. Very deep convolutional networks for large-scale image recognition. In *ICLR*, 2015.

Tan, T. J. L. and Shokri, R. Bypassing backdoor detection algorithms in deep learning. *arXiv preprint arXiv:1905.13409*, 2019.

Tran, B., Li, J., and Madry, A. Spectral signatures in backdoor attacks. In *NeurIPS*, 2018.

Turner, A., Tsipras, D., and Madry, A. Label-consistent backdoor attacks. *arXiv preprint arXiv:1912.02771*, 2019.

Wang, B., Yao, Y., Shan, S., Li, H., Viswanath, B., Zheng, H., and Zhao, B. Y. Neural cleanse: Identifying and mitigating backdoor attacks in neural networks. In *IEEE S&P*, 2019.

Zhang, T. Solving large scale linear prediction problems using stochastic gradient descent algorithms. In *ICML*, 2004.

Appendix

A. Settings for Studying the Effects of Trigger Characteristics

In this section, we illustrate the detailed settings in Section 3 of the main manuscript.

Attack Setup. We discuss the effects of trigger characteristics based on BadNets (Gu et al., 2019) in experiments. The trigger is a 3×3 black-gray square, as shown in Figure 3. The trade-off hyper-parameter α (see Eq. (1) in the main manuscript) is set as $\alpha \in \{0, 1\}^{3 \times 32 \times 32}$. The values of α entries corresponding to the pixels located in the minimum covering box are 1, while other values are 0.

Training Setup. We evaluate with two popular CNN models, including VGG-19 (Simonyan & Zisserman, 2015) and ResNet-34 (He et al., 2016), on the benchmark database CIFAR-10 (Krizhevsky et al., 2009). In terms of training, we adopt the SGD with momentum 0.9, weight decay 10^{-4} , and batch size 128 for all training processes. We train VGG-19 through 164 epochs with an initial learning rate of 0.1, which is decreased by a factor 10 at epochs 81 and 122; and train ResNet-34 through 300 epochs with an initial learning rate of 0.1, which is decreased by a factor 10 at epochs 150 and 250. The ratio of poisoned samples in training set, *i.e.*, $R = \frac{N_{poisoned}}{(N_{poisoned} + N_{benign})}$, is set to 0.25. All experiments are conducted on one single GeForce GTX 1080 GPU, and the implementation is conducted based on the open source code².

Data Preprocessing. Before adding a backdoor trigger to the benign sample to generate poisoned samples, we conduct standard data augmentation techniques for benign images. Specifically, 4-pixel padding is used before performing random crops of size 32×32 .

B. Settings for Transformation-based Defense

In this section, we illustrate the detailed settings in Section 5.1 of the main manuscript.

Defense Setup. We compare two special cases of the proposed transformation-based defense, *i.e.*, Flip and ShrinkPad, with representative state-of-the-art backdoor defenses, including fine-pruning (Liu et al., 2018), neural cleanse (Wang et al., 2019), and auto-encoder based defense (dubbed Auto-Encoder) (Liu et al., 2017b). Specifically, the fine-pruning method consists of two stages, including pruning and fine-tuning. Per the settings in the original paper, we prune the parameters of the last component (convolutional layer for VGG, convolutional block for ResNet). The origi-

²<https://github.com/bearpaw/pytorch-classification>

nal test set is equally divided as two disjoint subsets, including the validation set and the practical test set. The fraction of pruned neurons is determined through grid-search on the validation set, and the performance is evaluated on the practical test set. In particular, we found that the fine-tuning with even one epoch may reactivate the removed backdoor, therefore it is removed in the experiments. For neural cleanse, all settings are based on the open-source code³ provided by the authors. For Auto-Encoder, we train the convolutional auto-encoder (Geng et al., 2015) with 100 epochs, learning rate 0.001 and batch size 16. The implementation is based on the open-source code⁴.

Attack Setup. We use three representative state-of-the-art backdoor attacks, including BadNets (Gu et al., 2017), blended injection attack (Chen et al., 2017) (dubbed Blended Attack), and label consistent backdoor attack (Turner et al., 2019) (dubbed Consistent Attack) to evaluate the performance of backdoor defenses. The target label is *Deer*. Specifically, for BadNets, except for the trigger appearance, other settings are the same as those illustrated in Section A. The non-zero pixel value is modified from 128 to 255; For Blended Attack, the trigger is the same as the one of BadNets, the ratio of poisoned samples is set to 0.2, and the hyper-parameter $\alpha \in \{0, 0.2\}^{3 \times 32 \times 32}$. The values of the α entries corresponding to the pixels located in the minimum covering box are 0.2, while other values are 0; For Consistent Attack, the ratio of poisoned sample over all training samples with target label is set to 0.25, and $\alpha \in \{0, 0.25\}^{3 \times 32 \times 32}$. The trigger of Consistent Attack is quite different from the one used in BadNets and Blended Attack, which is symmetrical. All these settings follow their original papers. Some examples of poisoned sample generated by different attacks are shown in Figure 7.

Training Setup. The training settings here are the same as those stated in Section A.

C. Settings for Enhanced Attacks

In this section, we illustrate the detailed settings in Section 5.2 of the main manuscript.

Attack Setup. In the enhanced backdoor attacks, we adopt random Flip followed by random ShrinkPad in the random transformation layer. Note that there is only one hyper-parameter in enhanced attacks, *i.e.*, the maximal shrinking size, which is set to 4 pixels in this experiment. We examine three enhanced backdoor attacks, including enhanced BadNets (BadNet+), enhanced Blended Attack (Blended Attack+), and enhanced Consistent Attack (Consistent Attack+) with their correspondingly standard attack in the

experiments. In particular, when evaluating the ASR of enhanced attacks under defenses, the random transformation is also adopted on the benign training samples rather than only on the poisoned samples during the training process. This modification is to exclude the possibility that the transformation itself creates a new backdoor. For example, the zero-padding in ShrinkPad may probably create a new backdoor activated by the black edges of the image. If the random transformations are only adopted on the poisoned samples, we cannot identify whether the improvement of ASR under ShrinkPad is due to that the enhanced attacks are more robust to transformation, or due to that the black edges introduced by ShrinkPad activate the new edge-related backdoor of enhanced attacks.

Training Setup. The training settings here are the same as those stated in Section A.

D. Defense with Non-spatial Transformation

All transformations used for transformation-based defense in the main manuscript are spatial transformations (Flip and ShrinkPad). The spatial transformation could change the location and appearance of the trigger simultaneously. In this section, we also examine some non-spatial transformations, which only change the trigger appearance, while preserving its location. Specifically, we adopt the additive Gaussian noise and color-shifting.

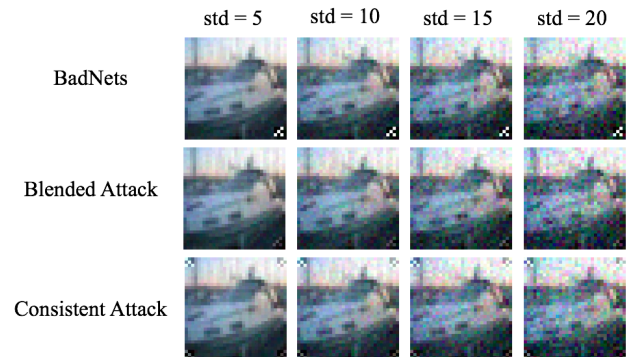


Figure 12. Transformed attacked samples with additive Gaussian noise.

Settings. We examine the performance of non-spatial transformation-based defense toward different backdoor attacks with ResNet-34 (see Section 5.1 of the main manuscript). For the additive Gaussian noise, the mean is set as zero, and the standard deviation (std), is selected from $\{\frac{5}{255}, \frac{10}{255}, \frac{15}{255}, \frac{20}{255}\}$. For the color-shifting, we examine four types of color-shifting, including modifying hue (dubbed Hue), modifying contrast (dubbed Contrast), modifying brightness (dubbed Brightness), and modifying saturation (dubbed Saturation). All images are randomly transformed with maximum perturbation size \in

³<https://github.com/bolunwang/backdoor>

⁴<https://github.com/jellycsc/>

PyTorch-CIFAR-10-autoencoder

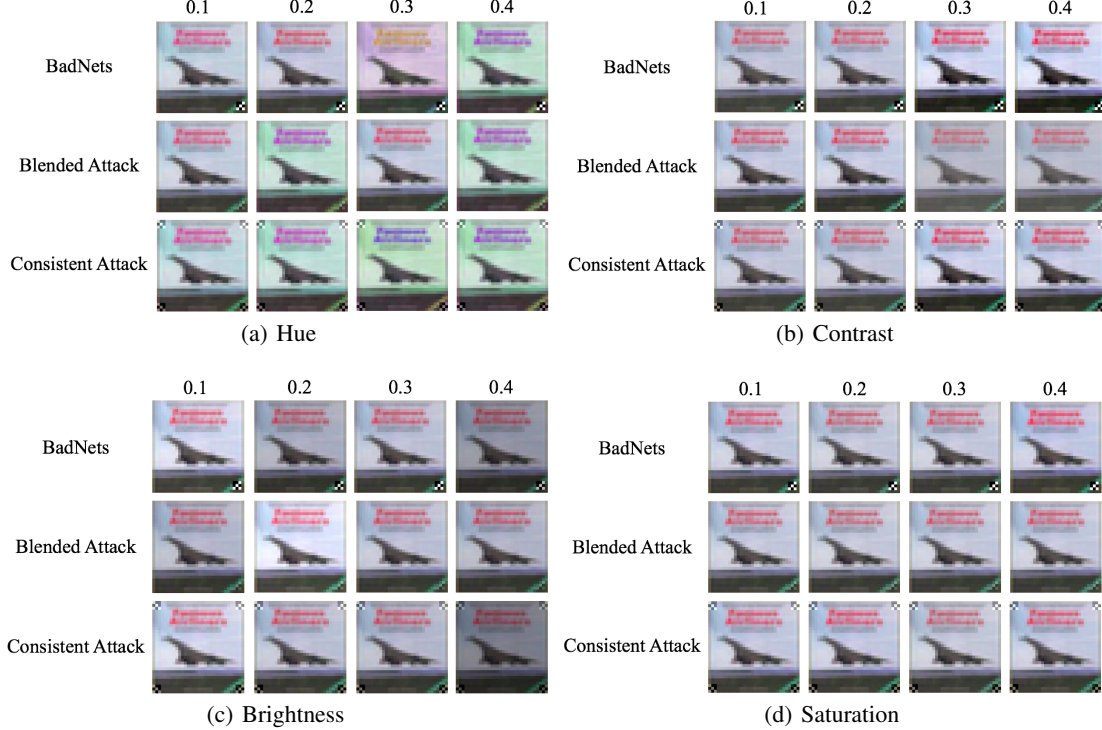


Figure 13. Transformed attacked samples with different types of color-shifting. All images are randomly transformed with maximum perturbation size $\in \{0.1, 0.2, 0.3, 0.4\}$.

Table 4. Attack success rate and clean test accuracy under additive Gaussian noise with different standard deviation.

Standard Deviation (std) \rightarrow	5		10		15		20	
Attack Type \downarrow	Clean	ASR	Clean	ASR	Clean	ASR	Clean	ASR
BadNets	91.2	100	79.8	100	58.1	100	36.4	100
Blended Attack	90.8	100	81.4	100	64.5	99.9	46.0	99.5
Consistent Attack	90.9	98.7	81.9	99.1	65.1	99.4	44.6	99.6

Table 5. Attack success rate and clean test accuracy under different types of color-shifting with different maximum perturbation sizes. We examine four types of color-shifting, including modifying hue (dubbed Hue), modifying contrast (dubbed Contrast), modifying brightness (dubbed Brightness), and modifying saturation (dubbed Saturation). All images are randomly transformed with maximum perturbation size $\in \{0.1, 0.2, 0.3, 0.4\}$.

Shifting Type \downarrow	Attack Type \downarrow	Maximum Perturbation Size \rightarrow		0.1		0.2		0.3		0.4	
		Clean	ASR	Clean	ASR	Clean	ASR	Clean	ASR	Clean	ASR
Hue	BadNets	93.2	100	91.6	100	89.4	100	88.5	100		
	Blended Attack	92.1	100	89.8	100	88	100	86.9	100		
	Consistent Attack	91.9	98.7	89.2	98.8	87.2	99	85.8	99.1		
Contrast	BadNets	94.2	100	94.0	100	93.8	100	93.7	100		
	Blended Attack	92.9	100	92.9	100	92.8	100	92.6	100		
	Consistent Attack	93.0	98.5	92.8	97.9	92.6	97.5	92.4	96.4		
Brightness	BadNets	94.1	100	93.9	100	93.7	100	93.4	100		
	Blended Attack	93.0	100	92.9	99.8	92.7	99.0	92.4	98.4		
	Consistent Attack	93.0	98.1	92.9	96.4	92.6	94.5	91.9	92.6		
Saturation	BadNets	94.1	100	94.1	100	94.1	100	94.0	100		
	Blended Attack	93.1	100	93.1	100	93.0	100	93.0	100		
	Consistent Attack	93.0	98.7	93.0	98.8	93.0	98.7	92.8	98.7		

$\{0.1, 0.2, 0.3, 0.4\}$, based on the *ColorJitter* function provided in torchvision. Some examples of transformed attacked images are shown in Figures 12 and 13.

As shown in Tables 4 and 5, both the additive Gaussian noise and color-shifting have limited effects on defending backdoor attacks. Especially for the additive Gaussian noise, despite the use of a large standard deviation, ASR has not

decreased even though the clean accuracy has decreased by more than 30%. The possible reason is that the effects of these transformations on the trigger appearance are not significant, as shown in Figures 12 and 13. Besides, the exact impact of the difference in trigger appearance on the attack success rate of backdoor attacks needs to be further studied in the future. Hence, in the proposed transformation-based defense, we recommend the spatial-transformations instead of non-spatial transformations.